

Neutrino Mass Predictions with an AI-based Algorithm under A_4 Modular Symmetry

Muhammad Waheed Aslam,^a Abrar Ahmad Zafar,^a Muhammad Naeem Aslam,^b

^a*Department of Physics, University of the Punjab, Lahore, Pakistan*

^b*Department of Mathematics, Lahore Garrison University, Lahore, Pakistan*

E-mail: waheed-979531@pu.edu.pk, waheed10aslam@gmail.com

ABSTRACT: This research undertakes a comprehensive exploration of neutrino mass model grounded in A_4 discrete non-Abelian modular symmetry formulated within a linear seesaw framework that modifies the conventional type-I seesaw structure with a focus on optimizing the model parameters using incomprehensible but intelligible-in-time logics optimization algorithm (ILA), an AI-based algorithm. In contrast to traditional discrete flavor symmetry frameworks, modular symmetry significantly reduces the number and complexity of flavon fields needed to generate realistic fermion mass textures. The key predictions include neutrino masses, U_{PMNS} matrices, effective neutrino masses for neutrinoless double beta decay, beta decay, Dirac and Majorana CP violation phases for normal (NO) and inverted mass ordering (IO), offering testable implications. The working efficiency of the ILA optimization technique is also estimated. The optimized neutrino oscillation parameters are well consistent with recent experimental data. Our analysis also aligns with Planck cosmological constraints on the sum of neutrino masses $0.06 < \Sigma m < 0.12$.

KEYWORDS: Modular Symmetry, Neutrino Masses and Mixing, Incomprehensible but Intelligible-in-time logics optimization Algorithm (ILA)

Contents

1	Introduction	1
2	Description of the Model under A_4 Modular based Model	3
3	IbI Logic Theory and the IbI Logic Algorithm (ILA)	5
3.1	Theoretical Foundations of IbI Logic	6
3.2	IbI Logic Algorithm (ILA)	7
3.2.1	Preparation Phase	7
3.2.2	Stage 1: Exploration	10
3.2.3	Stage 2: Integration	11
3.2.4	Stage 3: Exploitation	11
4	Numerical Analysis and Discussion	12
5	Conclusion	18

1 Introduction

Standard Model (SM) organizes quarks and leptons into three generations, yet offers no explanation for this family structure, the striking hierarchy of fermion masses, or the markedly different mixing patterns observed between leptons and quarks. Collectively, these open questions comprise the long-standing “flavor problem.”

Neutrinos, though feebly interacting and extraordinarily light, play a significant role in both particle physics and cosmology. They are copiously produced in stellar fusion [1], supernovae [2–6] and the Big Bang [7, 8] itself, and they underpin some of the greatest puzzles in modern science: the origin of neutrino mass [9], the nature of dark matter [10–14], the Higgs sector [15], and the cosmic matter–antimatter asymmetry [16]. The discovery of neutrino oscillations, first hinted at by the solar neutrino deficit and definitively demonstrated by Sudbury Neutrino Observatory (SNO) [17] and Super-Kamiokande [18], mandates nonzero neutrino masses and therefore physics beyond the SM.

Subsequent experiments such as KamLAND [19], OPERA [20], Daya Bay [21, 22], T2K [23], MINOS [24], NO ν A, and others) have further confirmed these oscillations and pinned down the two mass-squared differences and three mixing angles with impressive precision, given in NuFIT 6.0 [25] as shown in Table 1. However, the mass ordering, the octant of θ_{23} , and the CP-violating phases remain unsettled.

In the three active neutrino flavor, a theoretical framework to describe flavor mixing, provided by the PMNS matrix, a unitary matrix of dimension 3×3 , responsible for mixing the flavor eigenstates (ν_e , ν_μ , ν_τ) into the corresponding mass eigenstates (ν_1 , ν_2 , ν_3),

Parameters	Normal Ordering	Inverted Ordering
$\sin^2 \theta_{12}$	$0.275 \rightarrow 0.345$	$0.275 \rightarrow 0.345$
$\theta_{12}/^\circ$	$31.63 \rightarrow 35.95$	$31.63 \rightarrow 35.95$
$\sin^2 \theta_{23}$	$0.435 \rightarrow 0.585$	$0.437 \rightarrow 0.597$
$\theta_{23}/^\circ$	$41.3 \rightarrow 49.9$	$41.4 \rightarrow 50.6$
$\sin^2 \theta_{13}$	$0.020230 \rightarrow 0.02388$	$0.02053 \rightarrow 0.02397$
$\theta_{13}/^\circ$	$8.19 \rightarrow 8.89$	$8.24 \rightarrow 8.91$
$\delta_{CP}/^\circ$	$124 \rightarrow 364$	$201 \rightarrow 348$
$\frac{\Delta m_{21}^2}{10^{-5} eV^2}$	$6.92 \rightarrow 8.05$	$6.92 \rightarrow 8.05$
$\frac{\Delta m_{3l}^2}{10^{-3} eV^2}$	$+2.451 \rightarrow -2.584$	$0.275 \rightarrow -2.438$

Table 1. The table summarizes the best-fit values in 3σ range for neutrino oscillation parameters: mixing angles ($\sin^2 \theta_{12}$, $\sin^2 \theta_{23}$, $\sin^2 \theta_{13}$), mass-squared differences (Δm_{21}^2 and Δm_{3l}^2), and the δ_{CP} phase.

which possess masses m_1 , m_2 , and m_3 , respectively. The PMNS matrix can be parametrized through successive rotations and complex phases, with three mixing angles ($\theta_{12}, \theta_{23}, \theta_{13}$), a Dirac CP-violating phase (δ), and two Majorana phases (α, β) is given as [26]:

$$U_{PMNS} = U(\theta_{23}) U(\theta_{13}, \delta) U(\theta_{12}) U_M(\alpha, \beta) \\ = \begin{pmatrix} 1 & 0 & 0 \\ 0 & c_{23} & s_{23} \\ 0 & -s_{23} & c_{23} \end{pmatrix} \begin{pmatrix} c_{13} & 0 & s_{13}e^{-i\delta} \\ 0 & 1 & 0 \\ -s_{13}e^{i\delta} & 0 & c_{13} \end{pmatrix} \begin{pmatrix} c_{12} & s_{12} & 0 \\ -s_{12} & c_{12} & 0 \\ 0 & 0 & 1 \end{pmatrix} \begin{pmatrix} e^{i\alpha} & 0 & 0 \\ 0 & e^{i\beta} & 0 \\ 0 & 0 & 1 \end{pmatrix}. \quad (1.1)$$

Depending on the lightest mass and the sign of the larger mass-splitting, the spectrum may follow a NO or IO and can range from strongly hierarchical to quasi-degenerate. Oscillation experiments fix only mass-squared differences, while searches for neutrinoless double-beta decay probe the absolute mass scale and Majorana phases.

A compelling theoretical approach to the flavor problem invokes discrete non-Abelian symmetries, such as S_4 [27–32], A_4 [33–46], $\Delta(27)$ [47–53], and T_7 [54–64], to constrain the neutrino mass matrix and predict mixing angles and CP-violating phases.

More recently, modular symmetries [65–68], such as S_3 [69, 70], S_4 [71–73], A_4 [74–94], A_5 [95, 96], double covering of A_4 [97–99], S_4 [100, 101] and A_5 [102–104] have emerged as an elegant alternative where the Yukawa couplings themselves transform as modular forms τ that perform the role of flavons. When this modulus acquires the vacuum expectation value (VEV), it breaks the flavor symmetry, obviating the need for flavon fields. Here, τ is complex variable that is present in the Dedekind eta function $\eta(\tau)$ [105]. These frameworks yield highly predictive textures that can be confronted with data from current and upcoming oscillation experiments such as, JUNO [106], DUNE [107], Hyper-Kamiokande [108].

Realizing such models often leads to intricate parameter spaces and non-linear equations. AI-based algorithms have been widely used across various fields [109–147] and are being utilized in the context of neutrino phenomenology [148–150] have proven powerful in identifying best-fit regions consistent with experimental constraints.

In this work, we concentrate on an A_4 based modular construction [151] (augmented by a Type I seesaw) and employ Incomprehensible but Intelligible-in-time logics optimization algorithm (ILA) [152] to optimize its mixing parameters. Section 2 introduces the model and its field content; Sections 3 review the Incomprehensible but Intelligible-in-time logics: Theory and optimization algorithm; Section 4 presents our numerical results for both NO and IO, comparing them with the latest experimental and cosmological bounds; and Section 5 offers our concluding remarks.

2 Description of the Model under A_4 Modular based Model

We consider a model based on A_4 modular symmetry, an extension of SM within a linear seesaw framework, effectively modifying the type-I seesaw structure. In this framework, the Higgs and lepton superfields are transformed according to specific modular representations, as outlined in Table 2. The particle content is augmented by six singlet heavy superfields, N_{R_i} and S_{L_i} (both A_4 triplets), and a singlet weighton ρ . Modular Yukawa couplings, also A_4 triplets with weight $k_I = 2$, replace multiple flavon fields, preventing spectrum overpopulation and enhancing predictability. The VEVs of the Higgs superfields $\langle H_{u,d} \rangle = \frac{v_{u,d}}{\sqrt{2}}$ are connected to the VEV of the SM Higgs field through the relation $v_H = \sqrt{v_u^2 + v_d^2}$, where v_u and v_d denote the VEVs of H_u and H_d , respectively. The ratio of these VEVs is conventionally defined as $\tan \beta = (\frac{v_u}{v_d}) \approx 5$ [153–156].

Fields	e_R^c	μ_R^c	τ_R^c	$L_{\varphi L}$	N_R	S_L^c	$H_{u,d}$	ρ	$\mathbf{Y} = (y_1, y_2, y_3)$
$SU(2)_L$	1	1	1	2	1	1	2	1	–
$U(1)_Y$	1	1	1	$-\frac{1}{2}$	0	0	$\frac{1}{2}, -\frac{1}{2}$	0	–
$U(1)_X$	1	1	1	-1	1	-2	0	1	–
A_4	1	$1'$	$1''$	$1, 1'', 1'$	3	3	1	1	3
k_I	1	1	1	-1	-1	-1	0	0	2

Table 2. Particle content and Yukawa couplings under $SU(2)_L \times U(1)_Y \times U(1)_X \times A_4$ modular symmetry, where, k_I being the modular weight.

A global $U(1)_X$ symmetry [151] forbids unwanted superpotential terms. The A_4 symmetry is assumed to break above the electroweak scale [157], with $\langle \rho \rangle \neq 0$ generating masses for the new superfields. Suitable A_4 -singlet charge assignments for charged leptons yield a diagonal mass matrix matching observed values. Dirac M_D and pseudo-Dirac M_{LS} mass matrices arise from contractions of N_{R_i} and S_{L_i} with the triplet Yukawa coupling \mathbf{Y} respectively, while M_{RS} results from N_{R_i} and S_{L_i} mixing with $\alpha_{NS} \gg \beta_{NS}$. The super-potential of the model can be expressed as

$$\begin{aligned} \mathcal{W} = & y_\ell^{\varphi\varphi} L_{\varphi L} H_d \varphi_R^c + \alpha_D L_{\varphi L} H_u (\mathbf{Y} N_R)_{1,1'',1'} + \beta_D [L_{\varphi L} H_u (\mathbf{Y} S_L^c)_{1,1',1''}] \frac{\rho^3}{\Lambda^3} \\ & + [\alpha_{NS} \mathbf{Y} (S_L^c N_R)_{\text{sym}} + \beta_{NS} \mathbf{Y} (S_L^c N_R)_{\text{Anti-sym}}] \rho, \end{aligned} \quad (2.1)$$

The superpotential in Equation 2.1 involves diagonal matrices α_D and β_D with six free parameters, plus α_{NS} and β_{NS} . The Yukawa couplings $Y = (y_1, y_2, y_3)$, transforming as an A_4 triplet with modular weight 2, can be formulated using the Dedekind eta-function $\eta(\tau) = \sqrt[24]{q} \prod_{k=1}^{\infty} (1 - q^k)$ and its derivative with $q = \exp(2i\pi\tau)$, where q is a complex, are given as

$$\begin{aligned} y_1 &= \frac{i}{2\pi} \left(\frac{\eta'(\frac{\tau+1}{3})}{\eta(\frac{\tau+1}{3})} + \frac{\eta'(\frac{\tau+2}{3})}{\eta(\frac{\tau+2}{3})} + \frac{\eta'(\frac{\tau}{3})}{\eta(\frac{\tau}{3})} - \frac{27\eta'(3\tau)}{\eta(3\tau)} \right), \\ y_2 &= -\frac{i}{\pi} \left(\omega^2 \frac{\eta'(\frac{\tau+1}{3})}{\eta(\frac{\tau+1}{3})} + \omega \frac{\eta'(\frac{\tau+2}{3})}{\eta(\frac{\tau+2}{3})} + \frac{\eta'(\frac{\tau}{3})}{\eta(\frac{\tau}{3})} \right), \\ y_3 &= -\frac{i}{\pi} \left(\omega^2 \frac{\eta'(\frac{\tau+2}{3})}{\eta(\frac{\tau+2}{3})} + \omega \frac{\eta'(\frac{\tau+1}{3})}{\eta(\frac{\tau+1}{3})} + \frac{\eta'(\frac{\tau}{3})}{\eta(\frac{\tau}{3})} \right). \end{aligned} \quad (2.2)$$

The charged lepton mass matrix is inherently diagonal, arising from the transformation properties of the left-handed and right-handed charged leptons, which belong to singlet representations. Owing to the tensor product structure of the A_4 symmetry, the mass matrix of charged leptons takes the form, $M_\ell = \text{diag}(y_\ell^{ee} v_d/\sqrt{2}, y_\ell^{\mu\mu} v_d/\sqrt{2}, y_\ell^{\mu\mu} v_d/\sqrt{2}) = \text{diag}(m_e, m_\mu, m_\tau)$, with m_e , m_μ and m_τ denote the physical masses of the charged leptons [158]. The light neutrino mass matrix is

$$m_\nu = -M_D M_{RS}^{-1} M_{LS}^T + \text{ transpose} = \begin{pmatrix} M_{11} & M_{12} & M_{13} \\ M_{12} & M_{22} & M_{23} \\ M_{13} & M_{23} & M_{33} \end{pmatrix}, \quad (2.3)$$

with,

$$\begin{aligned} M_{11} = & (3\alpha_1\beta_1 v_u^2 v_\rho^2 (y_1^4 (\alpha_{NS} + 3\beta_{NS})^2 - 12y_2 y_3 y_1^2 \alpha_{NS} (\alpha_{NS} + 2\beta_{NS}) - 8(y_2^3 + y_3^3) y_1 \alpha_{NS}^2 \\ & - 36y_2^2 y_3^2 \beta_{NS}^2)) / (4\Lambda^3 (y_1^3 \alpha_{NS} (\alpha_{NS} + 3\beta_{NS})^2 - 3y_2 y_3 y_1 (\alpha_{NS} - 3\beta_{NS}) (2\alpha_{NS} \beta_{NS} \\ & + \alpha_{NS}^2 + 3\beta_{NS}^2) + (y_2^3 + y_3^3) \alpha_{NS} (\alpha_{NS}^2 - 9\beta_{NS}^2))), \end{aligned} \quad (2.4)$$

$$\begin{aligned} M_{12} = & -(3v_u^2 v_\rho^2 (2y_2 y_1^3 (\alpha_{NS} + 3\beta_{NS}) (\alpha_1 \beta_2 \alpha_{NS} + \alpha_2 \beta_1 (\alpha_{NS} - 3\beta_{NS})) + 9y_3^2 y_1^2 (\alpha_{NS} \\ & + \beta_{NS}) (\alpha_1 \beta_2 (\alpha_{NS} - \beta_{NS}) + \alpha_2 \beta_1 (\alpha_{NS} + \beta_{NS})) + 6y_2^2 y_3 y_1 (\alpha_2 \beta_1 + \alpha_1 \beta_2) (\alpha_{NS} \beta_{NS} \\ & + 2\alpha_{NS}^2 + 3\beta_{NS}^2) + 2y_2 (y_2^3 \alpha_{NS} (\alpha_2 \beta_1 (\alpha_{NS} + 3\beta_{NS}) + \alpha_1 \beta_2 (\alpha_{NS} - 3\beta_{NS})) \\ & + y_3^3 (\alpha_1 \beta_2 (\alpha_{NS} + 3\beta_{NS})^2 + \alpha_2 \beta_1 (\alpha_{NS} - 3\beta_{NS})^2))) / (8\Lambda^3 (y_1^3 \alpha_{NS} (\alpha_{NS} + 3\beta_{NS})^2 \\ & - 3y_2 y_3 y_1 (\alpha_{NS} - 3\beta_{NS}) (2\alpha_{NS} \beta_{NS} + \alpha_{NS}^2 + 3\beta_{NS}^2) \\ & + (y_2^3 + y_3^3) \alpha_{NS} (\alpha_{NS}^2 - 9\beta_{NS}^2))), \end{aligned} \quad (2.5)$$

$$\begin{aligned}
M_{13} = & - (3v_u^2 v_\rho^2 (2y_3 y_1^3 (\alpha_{NS} + 3\beta_{NS}) (\alpha_3 \beta_1 \alpha_{NS} + \alpha_1 \beta_3 (\alpha_{NS} - 3\beta_{NS})) + 9y_2^2 y_1^2 (\alpha_{NS} \\
& + \beta_{NS}) (\alpha_3 \beta_1 (\alpha_{NS} - \beta_{NS}) + \alpha_1 \beta_3 (\alpha_{NS} + \beta_{NS})) + 6y_2 y_3^2 y_1 (\alpha_3 \beta_1 + \alpha_1 \beta_3) \\
& (\alpha_{NS} \beta_{NS} + 2\alpha_{NS}^2 + 3\beta_{NS}^2) + 2y_3 (y_2^3 (\alpha_3 \beta_1 (\alpha_{NS} + 3\beta_{NS})^2 + \alpha_1 \beta_3 (\alpha_{NS} - 3\beta_{NS})^2) \\
& + y_3^3 \alpha_{NS} (\alpha_1 \beta_3 (\alpha_{NS} + 3\beta_{NS}) + \alpha_3 \beta_1 (\alpha_{NS} - 3\beta_{NS})))) / (8\Lambda^3 (y_1^3 \alpha_{NS} (\alpha_{NS} + 3\beta_{NS})^2 \\
& - 3y_2 y_3 y_1 (\alpha_{NS} - 3\beta_{NS}) (2\alpha_{NS} \beta_{NS} + \alpha_{NS}^2 + 3\beta_{NS}^2) \\
& + (y_2^3 + y_3^3) \alpha_{NS} (\alpha_{NS}^2 - 9\beta_{NS}^2))),
\end{aligned} \tag{2.6}$$

$$\begin{aligned}
M_{22} = & - (3\alpha_2 \beta_2 y_3 v_u^2 v_\rho^2 (4y_1^3 \alpha_{NS} (2\alpha_{NS} + 3\beta_{NS}) + 6y_2 y_3 y_1 (\alpha_{NS} \beta_{NS} + 2\alpha_{NS}^2 + 3\beta_{NS}^2) \\
& - y_3^3 (\alpha_{NS}^2 - 9\beta_{NS}^2) + 8y_3^3 \alpha_{NS}^2)) / (4\Lambda^3 (y_1^3 \alpha_{NS} (\alpha_{NS} + 3\beta_{NS})^2 - 3y_2 y_3 y_1 (\alpha_{NS} \\
& - 3\beta_{NS}) (2\alpha_{NS} \beta_{NS} + \alpha_{NS}^2 + 3\beta_{NS}^2) + (y_2^3 + y_3^3) \alpha_{NS} (\alpha_{NS}^2 - 9\beta_{NS}^2))),
\end{aligned} \tag{2.7}$$

$$\begin{aligned}
M_{23} = & - (3v_u^2 v_\rho^2 (2y_1^4 (\alpha_3 \beta_2 + \alpha_2 \beta_3) \alpha_{NS} (\alpha_{NS} + 3\beta_{NS}) + 6y_2 y_3 y_1^2 (\alpha_2 \beta_3 (\alpha_{NS} - \beta_{NS}) (2\alpha_{NS} \\
& + 3\beta_{NS}) + \alpha_3 \beta_2 (\alpha_{NS} \beta_{NS} + 2\alpha_{NS}^2 + 3\beta_{NS}^2)) + 2(y_2^3 + y_3^3) y_1 (\alpha_2 \beta_3 (\alpha_{NS} + 3\beta_{NS})^2 \\
& + \alpha_3 \beta_2 \alpha_{NS} (\alpha_{NS} - 3\beta_{NS})) + 9y_2^2 y_3^2 (\alpha_2 \beta_3 (\alpha_{NS} - \beta_{NS})^2 + \alpha_3 \beta_2 (\alpha_{NS} + \beta_{NS})^2))) \\
& / (8\Lambda^3 (y_1^3 \alpha_{NS} (\alpha_{NS} + 3\beta_{NS})^2 - 3y_2 y_3 y_1 (\alpha_{NS} - 3\beta_{NS}) (2\alpha_{NS} \beta_{NS} + \alpha_{NS}^2 + 3\beta_{NS}^2) \\
& + (y_2^3 + y_3^3) \alpha_{NS} (\alpha_{NS}^2 - 9\beta_{NS}^2))),
\end{aligned} \tag{2.8}$$

$$\begin{aligned}
M_{33} = & - (3\alpha_3 \beta_3 y_2 v_u^2 v_\rho^2 (4y_1^3 \alpha_{NS} (2\alpha_{NS} + 3\beta_{NS}) + 6y_2 y_3 y_1 (\alpha_{NS} \beta_{NS} + 2\alpha_{NS}^2 + 3\beta_{NS}^2) \\
& - y_2^3 (\alpha_{NS}^2 - 9\beta_{NS}^2) + 8y_3^3 \alpha_{NS}^2)) / (4\Lambda^3 (y_1^3 \alpha_{NS} (\alpha_{NS} \\
& + 3\beta_{NS})^2 - 3y_2 y_3 y_1 (\alpha_{NS} - 3\beta_{NS}) (2\alpha_{NS} \beta_{NS} + \alpha_{NS}^2 + 3\beta_{NS}^2) \\
& + (y_2^3 + y_3^3) \alpha_{NS} (\alpha_{NS}^2 - 9\beta_{NS}^2))).
\end{aligned} \tag{2.9}$$

Here, the structure of the mass matrices of M_D , M_{LS} , and M_{RS} are given as:

$$M_D = \frac{v_u}{\sqrt{2}} \begin{pmatrix} \alpha_1 & 0 & 0 \\ 0 & \alpha_2 & 0 \\ 0 & 0 & \alpha_3 \end{pmatrix} \begin{pmatrix} y_1 & y_3 & y_2 \\ y_2 & y_1 & y_3 \\ y_3 & y_2 & y_1 \end{pmatrix}_{LR}, \tag{2.10}$$

$$M_{LS} = \frac{v_u}{\sqrt{2}} \left(\frac{v_\rho}{\sqrt{2}\Lambda} \right)^3 \begin{pmatrix} \beta_1 & 0 & 0 \\ 0 & \beta_2 & 0 \\ 0 & 0 & \beta_3 \end{pmatrix} \begin{pmatrix} y_1 & y_3 & y_2 \\ y_2 & y_1 & y_3 \\ y_3 & y_2 & y_1 \end{pmatrix}_{LR}, \tag{2.11}$$

$$M_{RS} = \frac{v_\rho}{\sqrt{2}} \left[\frac{\alpha_{NS}}{3} \begin{pmatrix} 2y_1 & -y_3 & -y_2 \\ -y_3 & 2y_2 & -y_1 \\ -y_2 & -y_1 & 2y_3 \end{pmatrix}_{sym} + \beta_{NS} \begin{pmatrix} 0 & y_3 & -y_2 \\ -y_3 & 0 & y_1 \\ y_2 & -y_1 & 0 \end{pmatrix}_{asym} \right]. \tag{2.12}$$

3 IbI Logic Theory and the IbI Logic Algorithm (ILA)

This section presents an integrated and detailed exposition of the Incomprehensible but Intelligible-in-time (IbI) Logic theory along with its implementation in the form of the IbI

Logic Algorithm (ILA). The theory provides a philosophical and mathematical framework to recognize the value of currently disregarded ideas or solutions, which may become logical or optimal over time. The algorithm operationalizes this idea through a robust multi-stage metaheuristic method aimed at solving complex and nonlinear optimization problems.

3.1 Theoretical Foundations of IbI Logic

Traditional logic systems classify propositions as either logical or non-logical based on present understanding and evidence. However, scientific history is replete with ideas that were once considered implausible, only to be later accepted as foundational truths. Recognizing this evolutionary nature of logic, IbI Logic introduces a third classification: ideas that are currently incomprehensible or rejected but have the potential to be understood and validated in the future. IbI Logic is defined by three logical domains: General Logic (GL): Logic that is universally accepted without the need for specialized knowledge. Special Logic (SL): Logic that requires advanced knowledge or experience to be comprehended. IbI Logic: Logic that is currently considered invalid or non-logical but may emerge as logical with the evolution of understanding. To formalize the progression of an idea or solution from non-logic to logic, three principal metrics are introduced: C_i (Comprehensibility Index) represents the distance between the current solution and the accepted logical framework. D_i (Degree of Knowledge Shift) measures the amount of knowledge change from a prior iteration. P_i (Probability Index) reflects the likelihood that the candidate solution will become logical in the future. These quantities are calculated as follows:

$$C_i = \sqrt{\sum_{i=1}^{n_{NL}} (E_i - L)^2}, \quad (3.1)$$

$$D_i = \sqrt{\sum_{i=1}^{n_{NL}} (E_i - E_{i,p})^2}, \quad (3.2)$$

$$P_i = \sqrt{\sum_{i=1}^{n_{NL}} (E_i - EI_g)^2}, \quad (3.3)$$

where, E_i is current position (solution) of the i th expert, $E_{i,p}$ is previous position of the i th expert, L is logical solution or reference logic point and EI_g is best solution (elite) within the group.

To facilitate decision-making across different expert solutions, these values are normalized:

$$RC_i = \frac{C_i - C_{\min}}{C_{\max} - C_{\min}}, \quad (3.4)$$

$$RD_i = \frac{D_i - D_{\min}}{D_{\max} - D_{\min}}, \quad (3.5)$$

$$RP_i = \frac{P_i - P_{\min}}{P_{\max} - P_{\min}}, \quad (3.6)$$

where, RC_i , RD_i , RP_i are the normalized values of C_i , D_i , and P_i respectively. These parameters guide the transition of solutions across various phases of the algorithm.

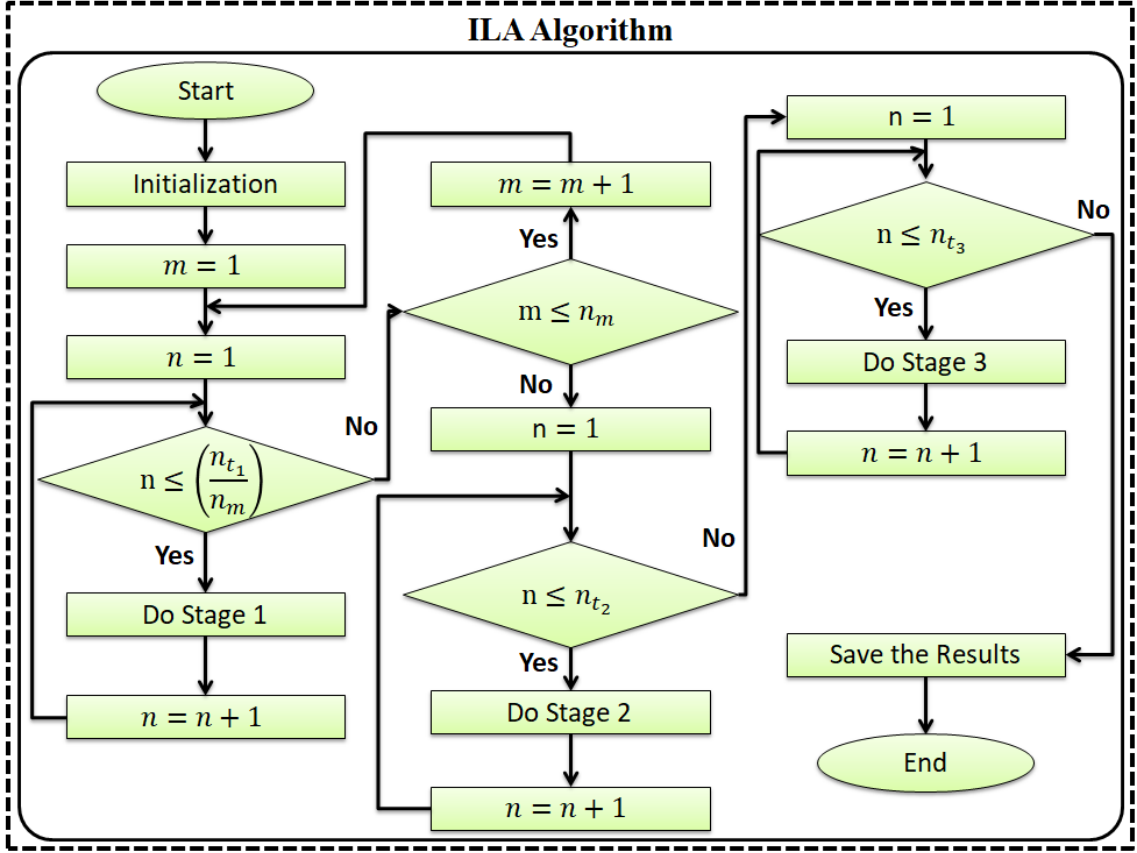


Figure 1. Generic flow of ILA

3.2 IbI Logic Algorithm (ILA)

The ILA is a nature-inspired metaheuristic optimization algorithm that models how initially non-logical solutions can evolve into optimal ones through iterative refinement and multi-level knowledge exchange. The algorithm consists of a Preparation Phase followed by three major stages: *Exploration*, *Integration*, and *Exploitation*. Each stage is designed to mimic different cognitive processes found in human reasoning. Figure 1 illustrates the working process of these three stages, and the pseudocode for each stage is presented in Figures 2, 3, and 4.

3.2.1 Preparation Phase

In the preparation phase, the total number of iterations N_T is divided among a predefined number of models n_m :

$$t_m = \frac{n_{t_1}}{n_m}, \quad (3.7)$$

$$n_{t_1} = p_{s_1} \cdot N_T, \quad (3.8)$$

where, n_{t_1} is the number of iterations assigned to stage 1, t_m is the number of iterations per model and p_{s_1} is the maximum percentage of iterations in stage 1. Each model is divided

Algorithm 1

Pseudocode for the preparation phase and stage 1

Input: $N_T, n_{NL}, n_m, B_{min}, B_{max}, p_{S1}, n_{g,max}, n_{rep}, n_{hep}, t_{clus}$
Initialization:

- Initialize the current NLs for the experts randomly $E_i(i = 1, \dots, n_{NL})$
 - Initialize the previous NLs for the experts randomly $E_{i,p}(i = 1, \dots, n_{NL})$
 - Determine the fitness $f(E_i)$ for E_i ; Set the best fitness as IbI
 - Determine the fitness $f(E_{i,p})$ for $E_{i,p}$; Set the best fitness as L
 - Choose the number of groups randomly in each class between 1 and $n_{g,max}$ as $n_{g,m}$
- for** $m = 1$ **to** n_m **do** ▷ (Preparation Phase)
- Do k-means clustering approach based on experts, $n_{g,m}, n_{rep}, n_{hep}, t_{clus}$
- Assign the specified clusters (groups) to the experts
- for** $n = 1$ **to** $(p_{S1} \cdot N_T)/n_m$ **do** ▷ (Start of the Stage 1)
- for** $g = 1$ **to** $n_{g,m}$ **do**
- Specify the best expert (an expert with the optimum fitness) of the g th group as $E_{I,g}$
- Specify the average between the experts of the g th group as $E_{a,g}$
- end for**
- for** $g = 1$ **to** $n_{g,m}$ **do**
- for** $i = 1$ **to** n_{NL} **do**
- if** $E_i \in g$ th group **then**
- Calculate R_C based on B_{min} and B_{max} using Eq. (3.4)
- Calculate R_D based on B_{min} and B_{max} using Eq. (3.5)
- Calculate R_P based on B_{min} and B_{max} using Eq. (3.6)
- end if**
- end for**
- end for**
- for** $i = 1$ **to** n_{NL} **do**
- if** $E_i \in g$ th group **then**
- Calculate KS_I using Eq. (3.16)
- Update E_i as $ES_{I,i}$ using Eq. (3.20)
- Update E_i, L , and $E_{p,i}$
- end if**
- end for**
- end for**
- end for**
- return** $ES_{I,i}(i = 1, \dots, n_{NL}), E_{p,i}(i = 1, \dots, n_{NL}), L, E_I$
-

Figure 2. Preparation and Stage 1 (Groupwork)

Algorithm 2

Pseudocode for stage 2**Input:** $ES_{1,i}(i = 1, \dots, n_{NL}), E_{p,i}(i = 1, \dots, n_{NL}), L, E_I, p_{S2}$ **for** $n = 1$ **to** $(p_{S2} \cdot N_T)$ **do** **for** $i = 1$ **to** n_{NL} **do** Specify the best expert (an expert with the optimum fitness) E_I Specify the average between the experts as E_A **end for** **for** $i = 1$ **to** n_{NL} **do** Calculate R_C based on B_{min} and B_{max} using Eq. (3.4) Calculate R_D based on B_{min} and B_{max} using Eq. (3.5) Calculate R_P based on B_{min} and B_{max} using Eq. (3.21) **end for** **for** $i = 1$ **to** n_{NL} **do** Calculate KS_2 using Eq. (3.28) Update E_i as $ES_{2,i}$ using Eq. (3.32) Update E_i, L , and $E_{p,i}$ **end for****end for****return** $ES_{2,i}(i = 1, \dots, n_{NL}), E_I$

Figure 3. The Stage 2 (Integration)

Algorithm 3

Pseudocode for the stage 3**Input:** $E_{i,S2}(i = 1, \dots, n_{NL}), E_I, n_3$ **for** $n = 1$ **to** n_3 **do** **for** $i = 1$ **to** n_{NL} **do** Specify the average between the experts as E_A Calculate KS_3 using Eqs. (3.33) and (3.34) Update E_i as $ES_{3,i}$ using Eq. (3.38) Update E_I **end for****end for****return** E_I

Figure 4. The Stage 3 (IbI Logic Search)

into a random number of groups:

$$n_{g,m} = \text{randi}(n_{g,max}), \quad m = 1, 2, 3, \dots, n_m \quad (3.9)$$

where, $n_{g,max}$ is the maximum number of groups in each model. These groups of experts explore solution spaces independently during the first stage.

3.2.2 Stage 1: Exploration

In this phase, each group of experts searches locally for potential solutions that may appear non-optimal at first but could evolve to be superior. Knowledge is constructed in two layers to guide this exploration.

Knowledge Layer 1 ($K0_{i,S1}$) This layer incorporates RC_i and RP_i to derive initial knowledge influence:

$$K0_{i,S1} = RP_i \cdot \frac{E_i + E_r}{2}, \quad \text{if } RC_i \leq BC, RP_i \leq BP, \quad (3.10)$$

$$K0_{i,S1} = RP_i \cdot \frac{E_i + A_g}{2}, \quad \text{if } RC_i \leq BC, RP_i > BP, \quad (3.11)$$

$$K0_{i,S1} = RP_i \cdot \frac{EI_g + E_r}{2}, \quad \text{if } RC_i > BC, RP_i \leq BP, \quad (3.12)$$

$$K0_{i,S1} = RP_i \cdot \frac{EI_g + A_g}{2}, \quad \text{if } RC_i > BC, RP_i > BP, \quad (3.13)$$

where, A_g is average position of the group and E_r is randomly selected expert solution.

Knowledge Layer 2 ($K1_{i,S1}$) This layer uses RD_i to evaluate the potential for deeper learning:

$$K1_{i,S1} = c_1 A_g, \quad \text{if } RD_i \leq BD, \quad (3.14)$$

$$K1_{i,S1} = c_1 E_u, \quad \text{if } RD_i > BD, \quad (3.15)$$

where, E_u is the uniform random solution in search space and BD , BC , BP are the thresholds for RD_i , RC_i , and RP_i used in knowledge decision rules. The total knowledge vector is:

$$K_{S1} = \frac{|K0_{S1} + K1_{S1}|}{2}. \quad (3.16)$$

Experts update their positions using:

$$E_{S1,new1} = E_i + c_2 K_{S1}, \quad (3.17)$$

$$E_{S1,new2} = c_3 E_{S1,new1} + c_4 EI_g, \quad (3.18)$$

$$E_{S1,new} = \min(E_{S1,new1}, E_{S1,new2}), \quad (3.19)$$

$$E_{i,S1} = \min(E_i, E_{S1,new}). \quad (3.20)$$

3.2.3 Stage 2: Integration

In the integration phase, all expert groups are merged and global knowledge is applied. This allows knowledge sharing across previously isolated domains. The probability index is recalculated as:

$$P_i = \sqrt{\sum_{i=1}^{n_{NL}} (E_i - EI)^2}, \quad (3.21)$$

where, EI is the global best (elite) solution across all groups. Updated knowledge layers:

$$K0_{i,S2} = RP_i \cdot \frac{E_i + E_R}{2}, \quad (3.22)$$

$$K0_{i,S2} = RP_i \cdot \frac{E_i + A}{2}, \quad (3.23)$$

$$K0_{i,S2} = RP_i \cdot \frac{EI + E_R}{2}, \quad (3.24)$$

$$K0_{i,S2} = RP_i \cdot \frac{EI + A}{2}, \quad (3.25)$$

$$K1_{i,S2} = c_5 A, \quad \text{if } RD_i \leq BD, \quad (3.26)$$

$$K1_{i,S2} = c_5 E_u, \quad \text{if } RD_i > BD, \quad (3.27)$$

where E_R is another reference expert or randomly selected elite solution and A is the global average of all expert solutions. Combined knowledge and updates:

$$K_{S2} = \frac{|K0_{S2} + K1_{S2}|}{2}, \quad (3.28)$$

$$E_{S2,new1} = E_i + c_6 K_{S2}, \quad (3.29)$$

$$E_{S2,new2} = c_7 E_{S2,new1} + c_8 EI, \quad (3.30)$$

$$E_{S2,new} = \min(E_{S2,new1}, E_{S2,new2}), \quad (3.31)$$

$$E_{i,S2} = \min(E_i, E_{S2,new}). \quad (3.32)$$

3.2.4 Stage 3: Exploitation

In the final stage, fine-tuning is performed to exploit the best solutions found so far. This is akin to local search refinement. Knowledge difference is calculated as:

$$K_{i,S3} = |A - E_R|, \quad \text{if factor} = 1 \quad (3.33)$$

$$K_{i,S3} = |A - EI|, \quad \text{if factor} = 2 \quad (3.34)$$

The expert positions are updated:

$$E_{S3,new1} = E_i + c_9 K_{S3}, \quad (3.35)$$

$$E_{S3,new2} = c_{10} E_{S3,new1} + c_{11} EI, \quad (3.36)$$

$$E_{S3,new} = \min(E_{S3,new1}, E_{S3,new2}), \quad (3.37)$$

$$E_{i,S3} = \min(E_i, E_{S3,new}), \quad (3.38)$$

where c_1, c_2, \dots, c_{11} are the constants that control the influence of knowledge and random terms. This detailed integration of IbI theory and ILA methodology provides a structured pathway from abstract non-logical solutions to actionable, optimized outcomes, simulating the temporal evolution of logic in human cognition.

4 Numerical Analysis and Discussion

In the framework where the charged lepton mass matrix is assumed to be diagonal, the effective light neutrino mass matrix m_ν , as derived previously, must be brought to a diagonal form through a unitary transformation governed by the, U_{PMNS} . This transformation renders the neutrino mass matrix diagonal, ensuring the relation:

$$m_\nu = U^* m_{\text{diag}} U^\dagger, \quad (4.1)$$

where $m_{\text{diag}} = \text{diag}(m_1, m_2, m_3)$ denotes the diagonal matrix composed of the physical masses of the three light neutrino mass eigenstates. Consequently, the neutrino mass eigenvalues are encapsulated within m_{diag} , and the matrix U encodes the mixing parameters that relate flavor and mass eigenstates.

$$m_{\text{diag}} = \begin{cases} \text{diag}(m_1, \sqrt{m_1^2 + \Delta m_{21}^2}, \sqrt{m_1^2 + \Delta m_{31}^2}), & \text{in NO} \\ \text{diag}(\sqrt{m_3^2 + \Delta m_{31}^2}, \sqrt{m_3^2 + \Delta m_{31}^2 + \Delta m_{21}^2}, m_3), & \text{in IO} \end{cases} \quad (4.2)$$

Incorporating the most recent global neutrino oscillation data from NuFIT 6.0 [25], the objective (or fitness) function, denoted as Δ' , is formulated by embedding equation 4.1 within its structure. This formulation ensures consistency with contemporary experimental observations and facilitates a data-driven analysis of the neutrino mass matrix.

$$\Delta' = \Delta'_1 + \Delta'_2 + \Delta'_3 + \Delta'_4 + \Delta'_5 + \Delta'_6, \quad (4.3)$$

with,

$$\begin{aligned} \Delta'_1 = & \left[\left(c_{13}^2 (e^{2i\delta} m_1 c_{12}^2 + e^{2i\alpha} m_2 s_{12}^2) + e^{2i\beta} m_3 s_{13}^2 \right) - \left((3\alpha_1 \beta_1 v_u^2 v_\rho^2 (y_1^4 (\alpha_{NS} + 3\beta_{NS})^2 \right. \right. \\ & - 12y_2 y_3 y_1^2 \alpha_{NS} (\alpha_{NS} + 2\beta_{NS}) - 8(y_2^3 + y_3^3) y_1 \alpha_{NS}^2 - 36y_2^2 y_3^2 \beta_{NS}^2)) \\ & / (4\Lambda^3 (y_1^3 \alpha_{NS} (\alpha_{NS} + 3\beta_{NS})^2 - 3y_2 y_3 y_1 (\alpha_{NS} - 3\beta_{NS}) (2\alpha_{NS} \beta_{NS} \\ & \left. \left. + \alpha_{NS}^2 + 3\beta_{NS}^2) + (y_2^3 + y_3^3) \alpha_{NS} (\alpha_{NS}^2 - 9\beta_{NS}^2))) \right) \right]^2, \end{aligned} \quad (4.4)$$

$$\begin{aligned}
\Delta'_2 = & \left[\left(c_{13} \left[e^{i\beta} m_3 s_{13} s_{23} - e^{2i\delta} m_1 c_{12} (c_{23} s_{12} + e^{-i\beta} c_{12} s_{13} s_{23}) + e^{2i\alpha} m_2 s_{12} (c_{12} c_{23} \right. \right. \right. \right. \\
& - e^{-i\beta} s_{12} s_{13} s_{23}) \left. \right] \left. \right) + \left((3v_u^2 v_\rho^2 (2y_2 y_1^3 (\alpha_{NS} + 3\beta_{NS}) (\alpha_1 \beta_2 \alpha_{NS} + \alpha_2 \beta_1 (\alpha_{NS} - 3\beta_{NS})) \right. \\
& + 9y_3^2 y_1^2 (\alpha_{NS} + \beta_{NS}) (\alpha_1 \beta_2 (\alpha_{NS} - \beta_{NS}) + \alpha_2 \beta_1 (\alpha_{NS} + \beta_{NS})) \\
& + 6y_2^2 y_3 y_1 (\alpha_2 \beta_1 + \alpha_1 \beta_2) (\alpha_{NS} \beta_{NS} + 2\alpha_{NS}^2 + 3\beta_{NS}^2) + 2y_2 (y_2^3 \alpha_{NS} (\alpha_2 \beta_1 (\alpha_{NS} \\
& + 3\beta_{NS}) + \alpha_1 \beta_2 (\alpha_{NS} - 3\beta_{NS})) + y_3^3 (\alpha_1 \beta_2 (\alpha_{NS} + 3\beta_{NS})^2 + \alpha_2 \beta_1 (\alpha_{NS} \\
& - 3\beta_{NS})^2)))/(8\Lambda^3 (y_1^3 \alpha_{NS} (\alpha_{NS} + 3\beta_{NS})^2 - 3y_2 y_3 y_1 (\alpha_{NS} - 3\beta_{NS}) (2\alpha_{NS} \beta_{NS} \\
& + \alpha_{NS}^2 + 3\beta_{NS}^2) + (y_2^3 + y_3^3) \alpha_{NS} (\alpha_{NS}^2 - 9\beta_{NS}^2))) \left. \right)^2, \\
\end{aligned} \tag{4.5}$$

$$\begin{aligned}
\Delta'_3 = & \left[\left(c_{13} (e^{-i\beta} c_{23} (e^{2i\beta} m_3 - e^{2i\delta} m_1 c_{12}^2 - e^{2i\alpha} m_2 s_{12}^2) s_{13} + (e^{2i\delta} m_1 - e^{2i\alpha} m_2) c_{12} s_{12} s_{23}) \right) \right. \\
& + \left((3v_u^2 v_\rho^2 (2y_3 y_1^3 (\alpha_{NS} + 3\beta_{NS}) (\alpha_3 \beta_1 \alpha_{NS} + \alpha_1 \beta_3 (\alpha_{NS} - 3\beta_{NS})) + 9y_2^2 y_1^2 (\alpha_{NS} + \beta_{NS}) \right. \\
& (\alpha_3 \beta_1 (\alpha_{NS} - \beta_{NS}) + \alpha_1 \beta_3 (\alpha_{NS} + \beta_{NS})) + 6y_2 y_3^2 y_1 (\alpha_3 \beta_1 + \alpha_1 \beta_3) (\alpha_{NS} \beta_{NS} + 2\alpha_{NS}^2 \\
& + 3\beta_{NS}^2) + 2y_3 (y_2^3 (\alpha_3 \beta_1 (\alpha_{NS} + 3\beta_{NS})^2 + \alpha_1 \beta_3 (\alpha_{NS} - 3\beta_{NS})^2) + y_3^3 \alpha_{NS} (\alpha_1 \beta_3 (\alpha_{NS} \\
& + 3\beta_{NS}) + \alpha_3 \beta_1 (\alpha_{NS} - 3\beta_{NS}))))/(8\Lambda^3 (y_1^3 \alpha_{NS} (\alpha_{NS} + 3\beta_{NS})^2 - 3y_2 y_3 y_1 (\alpha_{NS} \\
& - 3\beta_{NS}) (2\alpha_{NS} \beta_{NS} + \alpha_{NS}^2 + 3\beta_{NS}^2) + (y_2^3 + y_3^3) \alpha_{NS} (\alpha_{NS}^2 - 9\beta_{NS}^2))) \left. \right)^2, \\
\end{aligned} \tag{4.6}$$

$$\begin{aligned}
\Delta'_4 = & \left[\left(m_3 c_{13}^2 s_{23}^2 + e^{2i\delta} m_1 (c_{23} s_{12} + e^{-i\beta} c_{12} s_{13} s_{23})^2 + e^{2i\alpha} m_2 (c_{12} c_{23} - e^{-i\beta} s_{12} s_{13} s_{23})^2 \right) \right. \\
& + \left((3\alpha_2 \beta_2 y_3 v_u^2 v_\rho^2 (4y_1^3 \alpha_{NS} (2\alpha_{NS} + 3\beta_{NS}) + 6y_2 y_3 y_1 (\alpha_{NS} \beta_{NS} + 2\alpha_{NS}^2 + 3\beta_{NS}^2) \right. \\
& - y_3^3 (\alpha_{NS}^2 - 9\beta_{NS}^2) + 8y_2^3 \alpha_{NS}^2))/(4\Lambda^3 (y_1^3 \alpha_{NS} (\alpha_{NS} + 3\beta_{NS})^2 - 3y_2 y_3 y_1 (\alpha_{NS} \\
& - 3\beta_{NS}) (2\alpha_{NS} \beta_{NS} + \alpha_{NS}^2 + 3\beta_{NS}^2) + (y_2^3 + y_3^3) \alpha_{NS} (\alpha_{NS}^2 - 9\beta_{NS}^2))) \left. \right)^2, \\
\end{aligned} \tag{4.7}$$

$$\begin{aligned}
\Delta'_5 = & \left[\left(m_3 c_{13}^2 c_{23} s_{23} - e^{2i\delta} m_1 (-e^{-i\beta} c_{12} c_{23} s_{13} + s_{12} s_{23}) (c_{23} s_{12} + e^{-i\beta} c_{12} s_{13} s_{23}) \right. \right. \\
& - e^{2i\alpha} m_2 (e^{-i\beta} c_{23} s_{12} s_{13} + c_{12} s_{23}) (c_{12} c_{23} - e^{-i\beta} s_{12} s_{13} s_{23}) \left. \right) \right. \\
& + \left((3v_u^2 v_\rho^2 (2y_1^4 (\alpha_3 \beta_2 + \alpha_2 \beta_3) \alpha_{NS} (\alpha_{NS} + 3\beta_{NS}) + 6y_2 y_3 y_1^2 (\alpha_2 \beta_3 (\alpha_{NS} - \beta_{NS}) (2\alpha_{NS} \\
& + 3\beta_{NS}) + \alpha_3 \beta_2 (\alpha_{NS} \beta_{NS} + 2\alpha_{NS}^2 + 3\beta_{NS}^2)) + 2(y_2^3 + y_3^3) y_1 (\alpha_2 \beta_3 (\alpha_{NS} + 3\beta_{NS})^2 \\
& + \alpha_3 \beta_2 \alpha_{NS} (\alpha_{NS} - 3\beta_{NS})) + 9y_2^2 y_3^2 (\alpha_2 \beta_3 (\alpha_{NS} - \beta_{NS})^2 + \alpha_3 \beta_2 (\alpha_{NS} + \beta_{NS})^2)))/(8\Lambda^3 (y_1^3 \alpha_{NS} (\alpha_{NS} + 3\beta_{NS})^2 - 3y_2 y_3 y_1 (\alpha_{NS} - 3\beta_{NS}) (2\alpha_{NS} \beta_{NS} + \alpha_{NS}^2 + 3\beta_{NS}^2) \right. \\
& + (y_2^3 + y_3^3) \alpha_{NS} (\alpha_{NS}^2 - 9\beta_{NS}^2))) \left. \right)^2, \\
\end{aligned} \tag{4.8}$$

$$\begin{aligned} \Delta'_6 = & \left[\left(m_3 c_{13}^2 c_{23}^2 + e^{2i\alpha} m_2 (e^{-i\beta} c_{23} s_{12} s_{13} + c_{12} s_{23})^2 + e^{2i\delta} m_1 (e^{-i\beta} c_{12} c_{23} s_{13} - s_{12} s_{23})^2 \right) \right. \\ & + \left. \left((3\alpha_3 \beta_3 y_2 v_u^2 v_\rho^2 (4y_1^3 \alpha_{NS} (2\alpha_{NS} + 3\beta_{NS}) + 6y_2 y_3 y_1 (\alpha_{NS} \beta_{NS} + 2\alpha_{NS}^2 + 3\beta_{NS}^2) \right. \right. \\ & - y_2^3 (\alpha_{NS}^2 - 9\beta_{NS}^2) + 8y_3^3 \alpha_{NS}^2)) / (4\Lambda^3 (y_1^3 \alpha_{NS} (\alpha_{NS} \\ & + 3\beta_{NS})^2 - 3y_2 y_3 y_1 (\alpha_{NS} - 3\beta_{NS}) (2\alpha_{NS} \beta_{NS} + \alpha_{NS}^2 + 3\beta_{NS}^2) \\ & \left. \left. + (y_2^3 + y_3^3) \alpha_{NS} (\alpha_{NS}^2 - 9\beta_{NS}^2))) \right) \right]^2, \end{aligned} \quad (4.9)$$

In our analysis, the Dedekind eta function is evaluated by truncating the infinite product to $k = 20$, which provides sufficient numerical precision for the range of parameters considered. The best-fit values of the model parameters are optimized using ILA for NO and IO. The optimization process was carried out for 500 iterations, which constituted one independent run. Based on this iterative process, we obtained the optimal values for the fundamental model parameters, along with the neutrino mass eigenvalues given in Table 3 (4) for NO (IO). The lepton mixing matrices for both NO and IO are determined as

Parameters	Optimal Value	Parameters	Optimal Value
θ_{12}	32.1233°	θ_{13}	8.8288°
θ_{23}	41.3953°	δ	308.388°
α	49.9705°	β	-20.215°
v_ρ	51.945 TeV	Λ	988.3455 TeV
α_1	1×10^{-6}	α_2	1×10^{-5}
α_3	8.4746×10^{-6}	β_1	3.8601×10^{-3}
β_2	9.4487×10^{-3}	β_3	3.5853×10^{-3}
α_{NS}	0.4599	β_{NS}	6.7517×10^{-5}
τ	$0.3071 + 1.1993i$	y_1	$0.9977 + 5.9914 \times 10^{-3}i$
y_2	$-0.38793 - 0.29294i$	y_3	$-3.30908 \times 10^{-2} - 0.11370i$
m_1	3.8630 meV	m_2	9.4775 meV
m_3	50.2784 meV		

Table 3. The optimized parameters include $\alpha_1, \alpha_2, \alpha_3, \beta_1, \beta_2, \beta_3, \alpha_{NS}, \beta_{NS}, y_1, y_2, y_3, \tau$, VEVs of v_ρ , cut-off scale Λ , mixing angles ($\theta_{12}, \theta_{13}, \theta_{23}$), phases (α, β, δ), and neutrino masses (m_1, m_2, m_3) using ILA for NO, achieving an objective function minimum of 1.0909×10^{-28} .

follows:

$$|U_{PMNS}| = \begin{cases} \begin{pmatrix} 0.83687 & 0.52544 & 0.15348 \\ 0.48047 & 0.58497 & 0.65342 \\ 0.26228 & 0.61783 & 0.74128 \end{pmatrix}, & \text{in NO} \\ \begin{pmatrix} 0.81934 & 0.55505 & 0.14352 \\ 0.45278 & 0.56617 & 0.68880 \\ 0.35167 & 0.60941 & 0.71060 \end{pmatrix}, & \text{in IO} \end{cases} \quad (4.10)$$

The effective neutrino mass parameters [159–163] relevant to both beta decay $\langle m_\beta \rangle$

Parameters	Optimal Value	Parameters	Optimal Value
θ_{12}	34.115°	θ_{13}	8.2517°
θ_{23}	44.1076°	δ	271.239°
α	28.2367°	β	57.2958°
v_ρ	90.9062 TeV	Λ	796.8692 TeV
α_1	5.9000×10^{-6}	α_2	1.72015×10^{-6}
α_3	1.5885×10^{-6}	β_1	5.4228×10^{-3}
β_2	7.7386×10^{-3}	β_3	2.2965×10^{-3}
α_{NS}	0.44152	β_{NS}	3.19021×10^{-5}
τ	$0.5 + 1.1679i$	y_1	$0.99221 + 1.0535 \times 10^{-16}i$
y_2	$-0.25879 - 0.44815i$	y_3	$6.74707 \times 10^{-2} - 0.11686i$
m_1	50.628 meV	m_2	51.3624 meV
m_3	7.2937 meV		

Table 4. The optimized parameters include $\alpha_1, \alpha_2, \alpha_3, \beta_1, \beta_2, \beta_3, \alpha_{NS}, \beta_{NS}, y_1, y_2, y_3, \tau$, VEVs of v_ρ , cut-off scale Λ , mixing angles ($\theta_{12}, \theta_{13}, \theta_{23}$), phases (α, β, δ), and neutrino masses (m_1, m_2, m_3) using ILA for IO, achieving an objective function minimum of 0.8037×10^{-30} .

and neutrinoless double beta decay $\langle m_{ee} \rangle$ offer critical insights into the fundamental nature of neutrinos, including their mass scale and whether they are Majorana particles. These parameters are derived from the elements of the lepton mixing matrix U_{ei} (where $i = 1, 2, 3$) and the corresponding light neutrino mass eigenstates m_i . The mathematical expressions for $\langle m_\beta \rangle$ and $\langle m_{ee} \rangle$ are given below:

$$\langle m_{ee} \rangle = \left| \sum_{i=1}^3 U_{ei}^2 m_i \right|, \quad \langle m_\beta \rangle = \sqrt{\sum_{i=1}^3 |U_{ei}|^2 m_i^2}. \quad (4.11)$$

These expressions capture both the modulus-squared contributions to observable masses in beta decay experiments and the complex interference effects arising from CP-violating and Majorana phases in the context of neutrinoless double beta decay. Using the best-fit parameter values obtained through the ILA technique, we have computed the values of $\langle m_{ee} \rangle$ and $\langle m_\beta \rangle$ for both the NO and IO mass ordering scenarios. These values are based on the detailed structure of the PMNS matrix elements and the predicted light neutrino masses within our model framework.

$$\langle m_{ee} \rangle = \begin{cases} 0.8416 \text{ meV}, & \text{in NO} \\ 27.9219 \text{ meV}, & \text{in IO} \end{cases}, \quad \langle m_\beta \rangle = \begin{cases} 13.9880 \text{ meV}, & \text{in NO} \\ 50.3445 \text{ meV}, & \text{in IO} \end{cases}. \quad (4.12)$$

Our analysis demonstrates that the resulting effective mass parameters are well within the sensitivities of upcoming and planned experimental searches, such as those conducted by the LEGEND, nEXO, and KATRIN collaborations. Specifically, the predicted value of $\langle m_{ee} \rangle$ provides a testable signature in neutrinoless double beta decay, offering a pathway to distinguish between different mass hierarchies and to probe the CP-violating nature of neutrinos.

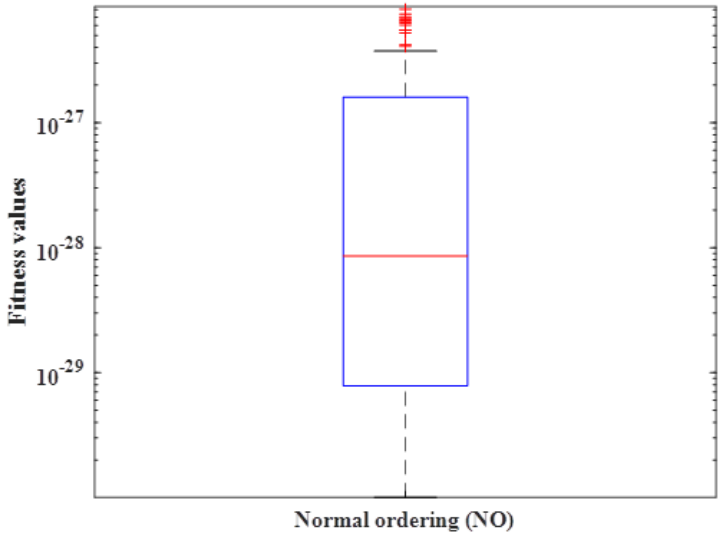


Figure 5. Boxplot of the fitness values obtained for the NO case.

In our study, we efficiently tuned the parameter space using ILA to get the optimal fit over 100 independent runs, each run having 600 iterations for both the hierarchy cases. ILA optimization has been demonstrated as being capable of navigating the complex, high-dimensional parameter space. It is well-suited to global optimization problems in which the objective function is nonlinear and possibly multi-modal. ILA was able to identify optimal parameter sets obeying experimental constraints on neutrino mixing angles, mass-squared differences, and CP-violating phases. The convergence accuracy of ILA was seen to reach around the benchmark of about 1.0909×10^{-28} (0.8037×10^{-30}) for NO (IO). Figures 5 and 6 show the boxplot of the fitness values for NO and IO. For NO, the vertical axis is shown on a logarithmic scale, ranging from 10^{-29} to 10^{-27} . The red horizontal line within the blue box denotes the median fitness value ($\sim 10^{-28}$), while the box boundaries represent the interquartile range containing the central 50% of the data. The whiskers extend to the most extreme data points within 1.5 times the interquartile range, and red crosses indicate outliers corresponding to poorer fits. The results show that the majority of solutions yield fitness values between $\sim 10^{-29}$ and $\sim 10^{-27}$, with the median located near 10^{-28} , demonstrating a generally good agreement with the imposed constraints, aside from a few higher-value outliers. For the IO case, Figure 6 shows that the fitness values span approximately from 10^{-31} to 10^{-28} , with the median located near 10^{-30} . The majority of solutions fall within this range, indicating a generally good fit to the constraints. A few outliers with higher fitness values ($\gtrsim 10^{-29}$) correspond to poorer fits.

An important metric for assessing the effectiveness and convergence behavior of the ILA algorithm is the evolution of the population distance across iterations, as depicted in Figures 7 and 8. The results demonstrate a consistent decrease in population distance, ultimately approaching zero. This trend indicates that the entire population is converging

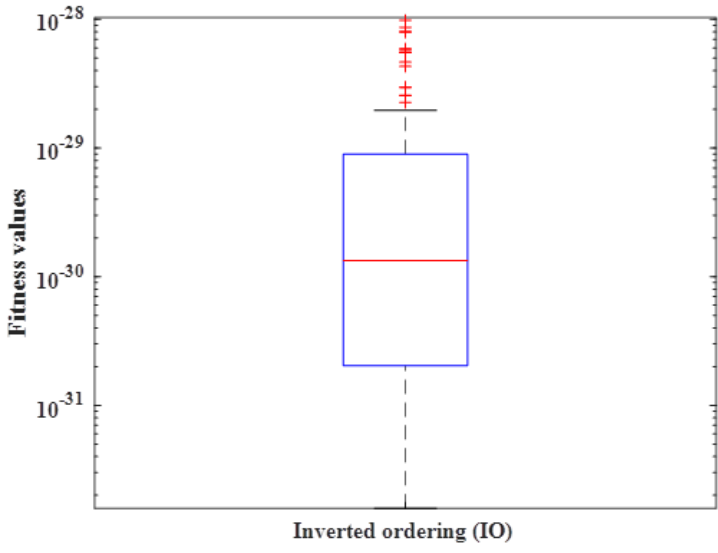


Figure 6. Boxplot of the fitness values obtained for the IO case.

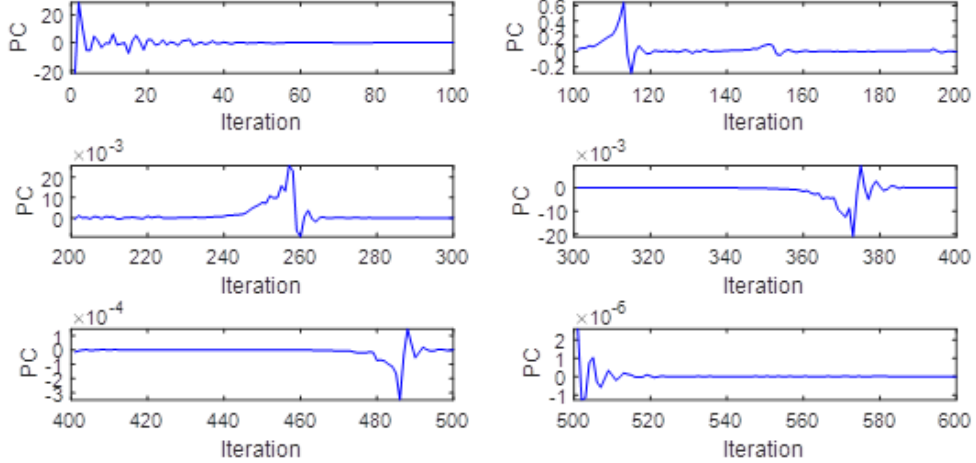


Figure 7. Best population convergence (PC) performance of ILA through iteration wise for NO

toward a common solution within the search space. Such a convergence suggests that the particles have collectively located a region of high fitness, with their velocities and positions becoming increasingly synchronized. The near-zero population distance provides strong empirical support for the algorithm's proper functioning and its efficient exploration of the solution landscape. This not only reflects the stability of the optimization process but also implies that the algorithm is likely converging to a global or near-global optimum. Consequently, the observed convergence behavior affirms both the robustness and reliability of the ILA methodology.

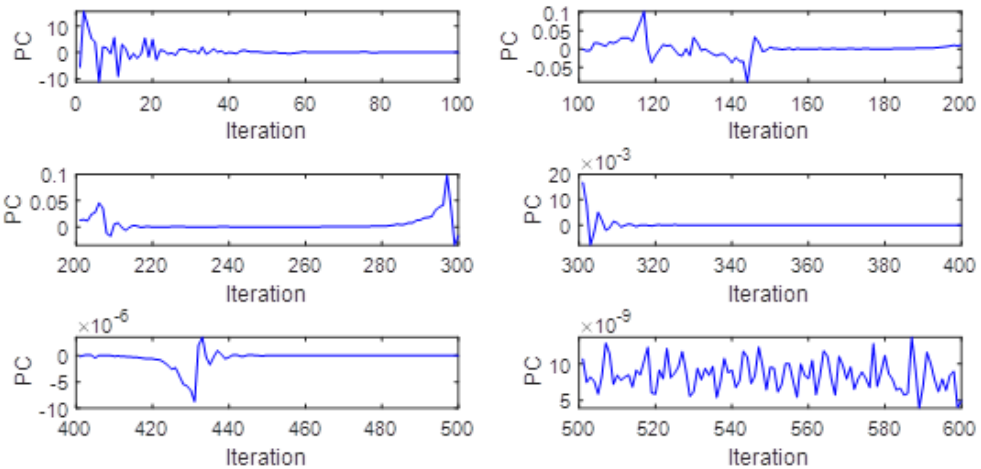


Figure 8. Best population convergence (PC) performance of ILA through iteration wise for IO

5 Conclusion

In this work, we have analyzed a comprehensive exploration of the neutrino mass model based on A_4 discrete non-Abelian modular symmetry formulated within a linear seesaw framework that modifies the conventional type-I seesaw structure with focus on optimizing the model parameters using incomprehensible but intelligible-in-time logics optimization algorithm (ILA), an AI-based algorithm. In this setup, the Higgs and lepton superfields transform under well-defined modular representations along with a singlet weighton ρ , allowing the flavor structure to be generated with a reduced number of flavon fields compared to conventional flavor models. This economy of fields avoids unnecessary spectrum proliferation while retaining the possibility of incorporating flavons, thereby improving both predictability and model-building flexibility. The effectiveness of ILA in computing the U_{PMNS} matrix and neutrino mass parameters is demonstrated for both NO and IO. For NO (IO), ILA produces neutrino masses as $m_1 = 3.8630 \text{ meV}$ ($m_1 = 50.628 \text{ meV}$), $m_2 = 9.4775 \text{ meV}$ ($m_2 = 51.3624 \text{ meV}$), $m_3 = 50.2784 \text{ meV}$ ($m_3 = 7.2937 \text{ meV}$), with effective neutrino mass parameters as $m_\beta = 13.9880 \text{ meV}$ ($m_\beta = 50.3445 \text{ meV}$), $m_{ee} = 0.8416 \text{ meV}$ ($m_{ee} = 27.9219 \text{ meV}$), demonstrating the robustness of ILA for precision modeling in neutrino mass scenarios. The model complies with the latest cosmological limit on the total neutrino mass, $\Sigma m_i \leq 0.12 \text{ eV}$, and also yields predictions for the mixing angles (θ_{ab} , $a < b$, $a, b \in \{1, 2, 3\}$), the Dirac phase δ , and the Majorana phases α and β , all in good agreement with current experimental data.

References

- [1] G.G. Raffelt, *Neutrinos and stars*, [1201.1637](#).
- [2] A. Burrows, *Neutrinos From Supernova Explosions*, *Ann. Rev. Nucl. Part. Sci.* **40** (1990) [181](#).

- [3] I. Tamborra and K. Murase, *Neutrinos from Supernovae*, *Space Sci. Rev.* **214** (2018) 31.
- [4] A. Burrows and T. Young, *Neutrinos and supernova theory*, *Phys. Rept.* **333** (2000) 63.
- [5] J. Cooperstein, *Neutrinos in Supernovae*, *Phys. Rept.* **163** (1988) 95.
- [6] M. Herant, S.A. Colgate, W. Benz and C. Fryer, *Neutrinos and supernovae*, *Los Alamos Science* **25** (1997) 64.
- [7] S. Sarkar, *Neutrinos from the Big Bang*, *arXiv e-prints* (2003) hep [[hep-ph/0302175](#)].
- [8] G. Steigman, *Neutrinos and Big Bang Nucleosynthesis*, *Physica Scripta Volume T* **121** (2005) 142 [[hep-ph/0501100](#)].
- [9] C. Weinheimer and K. Zuber, *Neutrino Masses*, *Annalen Phys.* **525** (2013) 565 [[1307.3518](#)].
- [10] M. Blennow, M. Carrigan and E. Fernandez Martinez, *Probing the Dark Matter mass and nature with neutrinos*, *Journal of Cosmology and Astroparticle Physics* **2013** (2013) 038 [[1303.4530](#)].
- [11] S.K. Agarwalla, M. Blennow, E. Fernandez Martinez and O. Mena, *Neutrino Probes of the Nature of Light Dark Matter*, *JCAP* **09** (2011) 004 [[1105.4077](#)].
- [12] S. Dodelson and L.M. Widrow, *Sterile neutrinos as dark matter*, *Physical Review Letters* **72** (1994) 17 [[hep-ph/9303287](#)].
- [13] G. Bertone and T. Tait, M. P., *A new era in the search for dark matter*, *Nature* **562** (2018) 51 [[1810.01668](#)].
- [14] D. Hooper and E.A. Baltz, *Strategies for Determining the Nature of Dark Matter*, *Ann. Rev. Nucl. Part. Sci.* **58** (2008) 293 [[0802.0702](#)].
- [15] S. Chakraborty and S. Roy, *Higgs boson mass, neutrino masses and mixing and keV dark matter in an $U(1)_R$ - lepton number model*, *Journal of High Energy Physics* **2014** (2014) 101 [[1309.6538](#)].
- [16] T2K collaboration, *Constraint on the matter–antimatter symmetry-violating phase in neutrino oscillations*, *Nature* **580** (2020) 339 [[1910.03887](#)].
- [17] SNO collaboration, *The Sudbury neutrino observatory*, *Nucl. Instrum. Meth. A* **449** (2000) 172 [[nucl-ex/9910016](#)].
- [18] Y. Fukuda, T. Hayakawa, E. Ichihara, K. Inoue, K. Ishihara, H. Ishino et al., *Evidence for Oscillation of Atmospheric Neutrinos*, *Physical Review Letters* **81** (1998) 1562 [[hep-ex/9807003](#)].
- [19] K. Eguchi, S. Enomoto, K. Furuno, J. Goldman, H. Hanada, H. Ikeda et al., *First Results from KamLAND: Evidence for Reactor Antineutrino Disappearance*, *Physical Review Letters* **90** (2003) 021802 [[hep-ex/0212021](#)].
- [20] R. Acquafredda, T. Adam, N. Agafonova, P. Alvarez Sanchez, M. Ambrosio, A. Anokhina et al., *The OPERA experiment in the CERN to Gran Sasso neutrino beam*, *Journal of Instrumentation* **04** (2009) 04018.
- [21] F.P. An, J.Z. Bai, A.B. Balantekin, H.R. Band, D. Beavis, W. Beriguete et al., *Observation of Electron-Antineutrino Disappearance at Daya Bay*, *Physical Review Letters* **108** (2012) 171803 [[1203.1669](#)].
- [22] F.P. An, A.B. Balantekin, H.R. Band, M. Bishai, S. Blyth, I. Butorov et al., *New*

Measurement of Antineutrino Oscillation with the Full Detector Configuration at Daya Bay, *Physical Review Letters* **115** (2015) 111802.

- [23] M.H. Ahn, E. Aliu, S. Andringa, S. Aoki, Y. Aoyama, J. Argyriades et al., *Measurement of neutrino oscillation by the K2K experiment*, *Physical Review D* **74** (2006) 072003 [[hep-ex/0606032](#)].
- [24] D.G. Michael, P. Adamson, T. Alexopoulos, W.W.M. Allison, G.J. Alner, K. Anderson et al., *Observation of Muon Neutrino Disappearance with the MINOS Detectors in the NuMI Neutrino Beam*, *Physical Review Letters* **97** (2006) 191801 [[hep-ex/0607088](#)].
- [25] I. Esteban, M. Gonzalez-Garcia, M. Maltoni, I. Martinez-Soler, J.P. Pinheiro and T. Schwetz, *NuFit-6.0: Updated global analysis of three-flavor neutrino oscillations*, *Journal of High Energy Physics* **2024** (2025) 1.
- [26] V.V. Vien, A.E. Cárcamo Hernández and H.N. Long, *The $\Delta(27)$ flavor 3-3-1 model with neutral leptons*, *Nuclear Physics B* **913** (2016) 792 [[1601.03300](#)].
- [27] T. Brown, S. Pakvasa, H. Sugawara and Y. Yamanaka, *Neutrino Masses, Mixing and Oscillations in $S(4)$ Model of Permutation Symmetry*, *Phys. Rev. D* **30** (1984) 255.
- [28] N. Chamoun and E.I. Lashin, *Textures of neutrino mass matrix from S_4 -flavor symmetry*, *JHEP* **01** (2025) 016 [[2308.10985](#)].
- [29] G.-J. Ding, J.-N. Lu, S.T. Petcov and B.-Y. Qu, *Non-holomorphic modular S_4 lepton flavour models*, *JHEP* **01** (2025) 191 [[2408.15988](#)].
- [30] T. Kobayashi, Y. Shimizu, K. Takagi, M. Tanimoto and T.H. Tatsuishi, *A_4 lepton flavor model and modulus stabilization from S_4 modular symmetry*, *Phys. Rev. D* **100** (2019) 115045 [[1909.05139](#)].
- [31] X.-G. Liu, C.-Y. Yao and G.-J. Ding, *Modular invariant quark and lepton models in double covering of S_4 modular group*, *Phys. Rev. D* **103** (2021) 056013 [[2006.10722](#)].
- [32] I. de Medeiros Varzielas, M. Levy, J.T. Penedo and S.T. Petcov, *Quarks at the modular S_4 cusp*, *JHEP* **09** (2023) 196 [[2307.14410](#)].
- [33] E. Ma and G. Rajasekaran, *Softly broken $A(4)$ symmetry for nearly degenerate neutrino masses*, *Phys. Rev. D* **64** (2001) 113012 [[hep-ph/0106291](#)].
- [34] M. Hirsch, S. Morisi and J.W.F. Valle, *A_4 -based tri-bimaximal mixing within inverse and linear seesaw schemes*, *Physics Letters B* **679** (2009) 454 [[0905.3056](#)].
- [35] M. Sruthilaya, R. Mohanta and S. Patra, *A_4 realization of linear seesaw and neutrino phenomenology*, *European Physical Journal C* **78** (2018) 719 [[1709.01737](#)].
- [36] D. Borah and B. Karmakar, *Linear seesaw for Dirac neutrinos with A_4 flavour symmetry*, *Physics Letters B* **789** (2019) 59 [[1806.10685](#)].
- [37] X.-G. He, Y.-Y. Keum and R.R. Volkas, *$A(4)$ flavor symmetry breaking scheme for understanding quark and neutrino mixing angles*, *JHEP* **04** (2006) 039 [[hep-ph/0601001](#)].
- [38] E. Ma, *Dark Scalar Doublets and Neutrino Tribimaximal Mixing from $A(4)$ Symmetry*, *Phys. Lett. B* **671** (2009) 366 [[0808.1729](#)].
- [39] G. Altarelli and D. Meloni, *A Simplest A_4 Model for Tri-Bimaximal Neutrino Mixing*, *J. Phys. G* **36** (2009) 085005 [[0905.0620](#)].
- [40] Y. Lin, *A Predictive $A(4)$ model, Charged Lepton Hierarchy and Tri-bimaximal Sum Rule*, *Nucl. Phys. B* **813** (2009) 91 [[0804.2867](#)].

- [41] Y.H. Ahn and C.-S. Chen, *Non-zero U_{e3} and TeV-Leptogenesis through A_4 symmetry breaking*, *Phys. Rev. D* **81** (2010) 105013 [[1001.2869](#)].
- [42] J. Barry and W. Rodejohann, *Deviations from tribimaximal mixing due to the vacuum expectation value misalignment in A_4 models*, *Phys. Rev. D* **81** (2010) 093002 [[1003.2385](#)].
- [43] V.V. Vien and H.N. Long, *Neutrino mixing with nonzero θ_{13} and CP violation in the 3-3-1 model based on A_4 flavor symmetry*, *Int. J. Mod. Phys. A* **30** (2015) 1550117 [[1405.4665](#)].
- [44] V.V. Vien, *Cobimaximal neutrino mixing in the $U(1)_{B-L}$ extension with A_4 symmetry*, *Mod. Phys. Lett. A* **35** (2020) 2050311.
- [45] G.-J. Ding, J.-N. Lu and J.W.F. Valle, *Trimaximal neutrino mixing from scotogenic A_4 family symmetry*, *Phys. Lett. B* **815** (2021) 136122 [[2009.04750](#)].
- [46] M. Dey, P. Chakraborty and S. Roy, *The μ - τ mixed symmetry and neutrino mass matrix*, *Phys. Lett. B* **839** (2023) 137767 [[2211.01314](#)].
- [47] G.C. Branco, J.M. Gerard and W. Grimus, *GEOMETRICAL T VIOLATION*, *Phys. Lett. B* **136** (1984) 383.
- [48] E. Ma, *Near tribimaximal neutrino mixing with Delta(27) symmetry*, *Phys. Lett. B* **660** (2008) 505 [[0709.0507](#)].
- [49] M. Abbas and S. Khalil, *Fermion masses and mixing in $\Delta(27)$ flavour model*, *Phys. Rev. D* **91** (2015) 053003 [[1406.6716](#)].
- [50] P. Chen, G.-J. Ding, A.D. Rojas, C.A. Vaquera-Araujo and J.W.F. Valle, *Warped flavor symmetry predictions for neutrino physics*, *JHEP* **01** (2016) 007 [[1509.06683](#)].
- [51] S. Centelles Chuliá, R. Srivastava and J.W.F. Valle, *CP violation from flavor symmetry in a lepton quarticity dark matter model*, *Phys. Lett. B* **761** (2016) 431 [[1606.06904](#)].
- [52] V.V. Vien and D.P. Khoi, *$U(1)$ $B-L$ extension based on $\Delta(27)$ symmetry for lepton masses and mixings*, *Mod. Phys. Lett. A* **35** (2020) 2050181.
- [53] A.E. Cárcamo Hernández, I. de Medeiros Varzielas, M.L. López-Ibáñez and A. Melis, *Controlled fermion mixing and FCNCs in a $\Delta(27)$ 3+1 Higgs Doublet Model*, *Journal of High Energy Physics* **2021** (2021) 215 [[2102.05658](#)].
- [54] C. Luhn, S. Nasri and P. Ramond, *Tri-bimaximal neutrino mixing and the family symmetry $Z_7 \rtimes Z_3$* , *Physics Letters B* **652** (2007) 27 [[0706.2341](#)].
- [55] C. Hagedorn, M.A. Schmidt and A.Y. Smirnov, *Lepton mixing and cancellation of the Dirac mass hierarchy in $SO(10)$ GUTs with flavor symmetries T_7 and $\Sigma(81)$* , *Physical Review D* **79** (2009) 036002 [[0811.2955](#)].
- [56] Q.-H. Cao, S. Khalil, E. Ma and H. Okada, *Observable T_7 Lepton Flavor Symmetry at the Large Hadron Collider*, *Physical Review Letters* **106** (2011) 131801 [[1009.5415](#)].
- [57] C. Luhn, K.M. Parattu and A. Wingerter, *A minimal model of neutrino flavor*, *Journal of High Energy Physics* **2012** (2012) 96 [[1210.1197](#)].
- [58] Y. Kajiyama, H. Okada and K. Yagyu, *T_7 flavor model in three loop seesaw and Higgs phenomenology*, *Journal of High Energy Physics* **2013** (2013) 196 [[1307.0480](#)].
- [59] C. Bonilla, S. Morisi, E. Peinado and J.W.F. Valle, *Relating quarks and leptons with the T_7 flavour group*, *Physics Letters B* **742** (2015) 99 [[1411.4883](#)].

- [60] V.V. Vien and H.N. Long, *The T_7 flavor symmetry in 3-3-1 model with neutral leptons*, *Journal of High Energy Physics* **2014** (2014) 133 [[1402.1256](#)].
- [61] V.V. Vien, *T_7 flavor symmetry scheme for understanding neutrino mass and mixing in 3-3-1 model with neutral leptons*, *Modern Physics Letters A* **29** (2014) 1450139 [[1508.02585](#)].
- [62] A.E. Cárcamo Hernández and R. Martínez, *Fermion mass and mixing pattern in a minimal T_7 flavor 331 model*, *Journal of Physics G: Nuclear and Particle Physics* **43** (2016) 45003 [[1511.07997](#)].
- [63] C. Arbeláez, A.E. Cárcamo Hernández, S. Kovalenko and I. Schmidt, *Adjoint $SU(5)$ GUT model with T_7 flavor symmetry*, *Physical Review D* **92** (2015) 115015 [[1507.03852](#)].
- [64] V.V. Vien and H.N. Long, *Fermion Mass and Mixing in a Simple Extension of the Standard Model Based on T_7 Flavor Symmetry*, *Physics of Atomic Nuclei* **82** (2019) 168.
- [65] G.K. Leontaris and N.D. Tracas, *Modular weights, $U(1)$'s and mass matrices*, *Phys. Lett. B* **419** (1998) 206 [[hep-ph/9709510](#)].
- [66] T. Kobayashi, K. Tanaka and T.H. Tatsuishi, *Neutrino mixing from finite modular groups*, *Phys. Rev. D* **98** (2018) 016004 [[1803.10391](#)].
- [67] F. Feruglio, *Are neutrino masses modular forms?*, in *From My Vast Repertoire ...: Guido Altarelli's Legacy*, A. Levy, S. Forte and G. Ridolfi, eds., pp. 227–266 (2019), DOI [[1706.08749](#)].
- [68] R. de Adelhart Toorop, F. Feruglio and C. Hagedorn, *Finite Modular Groups and Lepton Mixing*, *Nucl. Phys. B* **858** (2012) 437 [[1112.1340](#)].
- [69] S. Mishra, *Neutrino mixing and Leptogenesis with modular S_3 symmetry in the framework of type III seesaw*, [2008.02095](#).
- [70] H. Okada and Y. Orikasa, *Modular S_3 symmetric radiative seesaw model*, *Phys. Rev. D* **100** (2019) 115037 [[1907.04716](#)].
- [71] J.T. Penedo and S.T. Petcov, *Lepton Masses and Mixing from Modular S_4 Symmetry*, *Nucl. Phys. B* **939** (2019) 292 [[1806.11040](#)].
- [72] P.P. Novichkov, J.T. Penedo, S.T. Petcov and A.V. Titov, *Modular S_4 models of lepton masses and mixing*, *JHEP* **04** (2019) 005 [[1811.04933](#)].
- [73] H. Okada and Y. Orikasa, *Neutrino mass model with a modular S_4 symmetry*, [1908.08409](#).
- [74] T. Nomura, H. Okada and Y. Shoji, *$SU(4)_C \times SU(2)_L \times U(1)_R$ models with modular A_4 symmetry*, *PTEP* **2023** (2023) 023B04 [[2206.04466](#)].
- [75] M. Abbas, *Modular A_4 Invariance Model for Lepton Masses and Mixing*, *Phys. Atom. Nucl.* **83** (2020) 764.
- [76] T. Nomura and H. Okada, *Quark and lepton model with flavor specific dark matter and muon $g-2$ in modular A_4 and hidden $U(1)$ symmetries*, *Phys. Dark Univ.* **49** (2025) 101986 [[2304.13361](#)].
- [77] J. Kim and H. Okada, *Fermi-LAT GeV excess and muon $g-2$ in a modular A_4 symmetry*, [2302.09747](#).
- [78] M. Kashav and S. Verma, *On minimal realization of topological Lorentz structures with one-loop seesaw extensions in A_4 modular symmetry*, *JCAP* **03** (2023) 010 [[2205.06545](#)].

- [79] K.I. Nagao and H. Okada, *Lepton sector in modular A_4 and gauged $U(1)R$ symmetry*, *Nucl. Phys. B* **980** (2022) 115841 [[2010.03348](#)].
- [80] T. Asaka, Y. Heo and T. Yoshida, *Lepton flavor model with modular A_4 symmetry in large volume limit*, *Phys. Lett. B* **811** (2020) 135956 [[2009.12120](#)].
- [81] T. Nomura and H. Okada, *A linear seesaw model with A_4 -modular flavor and local $U(1)_{B-L}$ symmetries*, *JCAP* **09** (2022) 049 [[2007.04801](#)].
- [82] H. Okada and Y. Shoji, *A radiative seesaw model with three Higgs doublets in modular A_4 symmetry*, *Nucl. Phys. B* **961** (2020) 115216 [[2003.13219](#)].
- [83] M.K. Behera, S. Singirala, S. Mishra and R. Mohanta, *A modular A_4 symmetric scotogenic model for neutrino mass and dark matter*, *J. Phys. G* **49** (2022) 035002 [[2009.01806](#)].
- [84] G.-J. Ding, S.F. King and X.-G. Liu, *Modular A_4 symmetry models of neutrinos and charged leptons*, *JHEP* **09** (2019) 074 [[1907.11714](#)].
- [85] G. Altarelli and F. Feruglio, *Tri-bimaximal neutrino mixing, $A(4)$ and the modular symmetry*, *Nucl. Phys. B* **741** (2006) 215 [[hep-ph/0512103](#)].
- [86] M. Kashav and S. Verma, *Broken scaling neutrino mass matrix and leptogenesis based on A_4 modular invariance*, *JHEP* **09** (2021) 100 [[2103.07207](#)].
- [87] M.R. Devi, *Retrieving texture zeros in 3+1 active-sterile neutrino framework under the action of A_4 modular-invariants*, [2303.04900](#).
- [88] M.K. Singh, S.R. Singh and N.N. Singh, *Modular A_4 symmetry in 3+1 active-sterile neutrino masses and mixings*, *Int. J. Mod. Phys. A* **39** (2024) 2450145 [[2303.10922](#)].
- [89] S. Kikuchi, T. Kobayashi, K. Nasu, S. Takada and H. Uchida, *Quark mass hierarchies and CP violation in $A_4 \times A_4 \times A_4$ modular symmetric flavor models*, *JHEP* **07** (2023) 134 [[2302.03326](#)].
- [90] S.T. Petcov and M. Tanimoto, *A_4 modular flavour model of quark mass hierarchies close to the fixed point $\tau = \omega$* , *Eur. Phys. J. C* **83** (2023) 579 [[2212.13336](#)].
- [91] X.K. Du and F. Wang, *Flavor structures of quarks and leptons from flipped $SU(5)$ GUT with A_4 modular flavor symmetry*, *JHEP* **01** (2023) 036 [[2209.08796](#)].
- [92] G.-J. Ding, S.F. King, J.-N. Lu and B.-Y. Qu, *Leptogenesis in $SO(10)$ models with A_4 modular symmetry*, *JHEP* **10** (2022) 071 [[2206.14675](#)].
- [93] T. Nomura, H. Okada and Y.-h. Qi, *Zee model in a modular A_4 symmetry*, *Eur. Phys. J. C* **85** (2025) 134 [[2111.10944](#)].
- [94] H. Kuranaga, H. Ohki and S. Uemura, *Modular origin of mass hierarchy: Froggatt-Nielsen like mechanism*, *JHEP* **07** (2021) 068 [[2105.06237](#)].
- [95] P.P. Novichkov, J.T. Penedo, S.T. Petcov and A.V. Titov, *Modular A_5 symmetry for flavour model building*, *JHEP* **04** (2019) 174 [[1812.02158](#)].
- [96] C.-Y. Yao, X.-G. Liu and G.-J. Ding, *Fermion masses and mixing from the double cover and metaplectic cover of the A_5 modular group*, *Phys. Rev. D* **103** (2021) 095013 [[2011.03501](#)].
- [97] X.-G. Liu and G.-J. Ding, *Neutrino Masses and Mixing from Double Covering of Finite Modular Groups*, *JHEP* **08** (2019) 134 [[1907.01488](#)].
- [98] P. Beneš, H. Okada and Y. Oriksa, *Towards unification of lepton and quark mass matrices from double covering of modular A_4 flavor symmetry*, [2212.07245](#).

- [99] H. Okada and Y. Orikasa, *Lepton mass matrix from double covering of A_4 modular flavor symmetry**, *Chin. Phys. C* **46** (2022) 123108 [[2206.12629](#)].
- [100] Y. Abe, T. Higaki, J. Kawamura and T. Kobayashi, *Quark and lepton hierarchies from S_4' modular flavor symmetry*, *Phys. Lett. B* **842** (2023) 137977 [[2302.11183](#)].
- [101] Y. Abe, T. Higaki, J. Kawamura and T. Kobayashi, *Quark masses and CKM hierarchies from S'_4 modular flavor symmetry*, *Eur. Phys. J. C* **83** (2023) 1140 [[2301.07439](#)].
- [102] X. Wang, B. Yu and S. Zhou, *Double covering of the modular A_5 group and lepton flavor mixing in the minimal seesaw model*, *Phys. Rev. D* **103** (2021) 076005 [[2010.10159](#)].
- [103] M.K. Behera and R. Mohanta, *Linear Seesaw in A_5' Modular Symmetry With Leptogenesis*, *Front. in Phys.* **10** (2022) 854595 [[2201.10429](#)].
- [104] M.K. Behera and R. Mohanta, *Inverse seesaw in A'_5 modular symmetry*, *J. Phys. G* **49** (2022) 045001 [[2108.01059](#)].
- [105] S. Abbott, *Modular functions and dirichlet series in number theory, by tm apostol. pp 204. dm98. 1990. isbn 3-540-97127-0 (springer)*, *The Mathematical Gazette* **75** (1991) 249.
- [106] JUNO collaboration, *Neutrino Physics with JUNO*, *J. Phys. G* **43** (2016) 030401 [[1507.05613](#)].
- [107] DUNE collaboration, *Deep Underground Neutrino Experiment (DUNE), Far Detector Technical Design Report, Volume II: DUNE Physics*, [2002.03005](#).
- [108] HYPER-KAMIOKANDE collaboration, *Physics potentials with the second Hyper-Kamiokande detector in Korea*, *PTEP* **2018** (2018) 063C01 [[1611.06118](#)].
- [109] N.B. Guedria, *Improved accelerated PSO algorithm for mechanical engineering optimization problems*, *Applied Soft Computing* **40** (2016) 455.
- [110] A. Kaveh and E.A. NASR, *Engineering design optimization using a hybrid pso and hs algorithm*, .
- [111] N. Kumar, S.K. Mahato and A.K. Bhunia, *Design of an efficient hybridized CS-PSO algorithm and its applications for solving constrained and bound constrained structural engineering design problems*, *Results in Control and Optimization* **5** (2021) 100064.
- [112] S. Djemame, M. Batouche, H. Oulhadj and P. Siarry, *Solving reverse emergence with quantum PSO application to image processing*, *Soft Computing* **23** (2019) 6921.
- [113] R.P. Singh, M. Dixit and S. Silakari, *Image contrast enhancement using GA and PSO: a survey*, in *2014 International Conference on Computational Intelligence and Communication Networks*, pp. 186–189, IEEE, 2014.
- [114] J. Pramanik, S. Dalai and D. Rana, *Image registration using PSO and APSO: a comparative analysis*, *International Journal of Computer Applications* **116** (2015) .
- [115] F.Z. Azayite and S. Achhab, *Financial Early Warning System Model Based on Neural Networks, PSO and SA Algorithms*, in *EngOpt 2018 Proceedings of the 6th International Conference on Engineering Optimization*, pp. 970–982, Springer, 2019.
- [116] S.C. Chiam, K.C. Tan and A.A. Mamun, *A memetic model of evolutionary PSO for computational finance applications*, *Expert Systems with Applications* **36** (2009) 3695.
- [117] Y. Pan et al., *Design of financial management model using the forward neural network based on particle swarm optimization algorithm*, *Computational Intelligence and Neuroscience* **2022** (2022) .

- [118] Y. Marinakis, M. Marinaki, M. Doumpos and C. Zopounidis, *Ant colony and particle swarm optimization for financial classification problems*, *Expert Systems with Applications* **36** (2009) 10604.
- [119] M. Meissner, M. Schmuker and G. Schneider, *Optimized Particle Swarm Optimization (OPSO) and its application to artificial neural network training*, *BMC bioinformatics* **7** (2006) 1.
- [120] H.T. Rauf, W.H. Bangyal, J. Ahmad and S.A. Bangyal, *Training of artificial neural network using pso with novel initialization technique*, in *2018 international conference on innovation and intelligence for informatics, computing, and technologies (3ICT)*, pp. 1–8, IEEE, 2018.
- [121] A.A. Esmin, R.A. Coelho and S. Matwin, *A review on particle swarm optimization algorithm and its variants to clustering high-dimensional data*, *Artificial Intelligence Review* **44** (2015) 23.
- [122] S. Rana, S. Jasola and R. Kumar, *A review on particle swarm optimization algorithms and their applications to data clustering*, *Artificial Intelligence Review* **35** (2011) 211.
- [123] A. Stacey, M. Jancic and I. Grundy, *Particle swarm optimization with mutation*, .
- [124] R. Eberhart and J. Kennedy, *A new optimizer using particle swarm theory*, .
- [125] Q. He, L. Wang and B. Liu, *Parameter estimation for chaotic systems by particle swarm optimization*, *Chaos, Solitons & Fractals* **34** (2007) 654.
- [126] B. Alatas, E. Akin and A.B. Ozer, *Chaos embedded particle swarm optimization algorithms*, *Chaos, Solitons & Fractals* **40** (2009) 1715.
- [127] D. Babazadeh, M. Boroushaki and C. Lucas, *Optimization of fuel core loading pattern design in a VVER nuclear power reactors using Particle Swarm Optimization (PSO)*, *Annals of nuclear energy* **36** (2009) 923.
- [128] A.M. Ibrahim and M.A. Tawhid, *A hybridization of cuckoo search and particle swarm optimization for solving nonlinear systems*, *Evolutionary Intelligence* **12** (2019) 541.
- [129] P. Subbaraj and P. Rajnarayanan, *Hybrid particle swarm optimization based optimal reactive power dispatch*, *International Journal of Computer Applications* **1** (2010) 65.
- [130] A. Jiang, Y. Osamu and L. Chen, *Multilayer optical thin film design with deep Q learning*, *Scientific reports* **10** (2020) 12780.
- [131] C. Yue, Z. Qin, Y. Lang and Q. Liu, *Determination of thin metal film's thickness and optical constants based on SPR phase detection by simulated annealing particle swarm optimization*, *Optics Communications* **430** (2019) 238.
- [132] R.I. Rabady and A. Ababneh, *Global optimal design of optical multilayer thin-film filters using particle swarm optimization*, *Optik* **125** (2014) 548.
- [133] Z.-H. Ruan, Y. Yuan, X.-X. Zhang, Y. Shuai and H.-P. Tan, *Determination of optical properties and thickness of optical thin film using stochastic particle swarm optimization*, *Solar Energy* **127** (2016) 147.
- [134] A. Mehmood, A. Zameer, M.A.Z. Raja, R. Bibi, N.I. Chaudhary and M.S. Aslam, *Nature-inspired heuristic paradigms for parameter estimation of control autoregressive moving average systems*, *Neural Computing and Applications* **31** (2019) 5819.
- [135] Y. Yetis and M. Jamshidi, *Forecasting of Turkey's electricity consumption using Artificial Neural Network*, .

- [136] I.M. Yassin, A. Zabidi, M.S. Amin Megat Ali, N. Md Tahir, H. Zainol Abidin and Z.I. Rizman, *Binary particle swarm optimization structure selection of nonlinear autoregressive moving average with exogenous inputs (NARMAX) model of a flexible robot arm*, *International Journal on Advanced Science, Engineering and Information Technology* **6** (2016) 630.
- [137] S. Akbar, F. Zaman, M. Asif, A.U. Rehman and M.A.Z. Raja, *Novel application of FO-DPSO for 2-D parameter estimation of electromagnetic plane waves*, *Neural Computing and Applications* **31** (2019) 3681.
- [138] M.A. Fawzi, A.A. El-Fergany and H.M. Hasanien, *Effective methodology based on neural network optimizer for extracting model parameters of PEM fuel cells*, *International Journal of Energy Research* **43** (2019) 8136 .
- [139] M.S. AbouOmar, Y.X. Su, H. Zhang, B. Shi and L. li Wan, *Observer-based interval type-2 fuzzy PID controller for PEMFC air feeding system using novel hybrid neural network algorithm-differential evolution optimizer*, *Alexandria Engineering Journal* (2022) .
- [140] M.N. Aslam, M.W. Aslam, M.S. Arshad, Z. Afzal, M.K. Hassani, A.M. Zidan et al., *Neuro-computing solution for Lorenz differential equations through artificial neural networks integrated with PSO-NNA hybrid meta-heuristic algorithms: a comparative study*, *Scientific Reports* **14** (2024) .
- [141] F.A.J. Shaban, *NNA and Activation Equation-Based Prediction of New COVID-19 Infections*, *2023 5th International Congress on Human-Computer Interaction, Optimization and Robotic Applications (HORA)* (2023) 1.
- [142] Y. Zhang, Z. Jin and Y. Chen, *Hybrid teaching-learning-based optimization and neural network algorithm for engineering design optimization problems*, *Knowl. Based Syst.* **187** (2020) .
- [143] Y. Zhang, *Neural Network Algorithm With Reinforcement Learning for Parameters Extraction of Photovoltaic Models*, *IEEE Transactions on Neural Networks and Learning Systems* **34** (2021) 2806.
- [144] K. Qadeer, A. Ahmad, A. Naquash, M.A. Qyyum, K. Majeed, Z. Zhou et al., *Neural network-inspired performance enhancement of synthetic natural gas liquefaction plant with different minimum approach temperatures*, *Fuel* (2022) .
- [145] Y. Zhang, C. Huang, H. Huang and J. Wu, *Multiple Learning Neural Network Algorithm for Parameter Estimation of Proton Exchange Membrane Fuel Cell Models*, *Green Energy and Intelligent Transportation* (2022) .
- [146] M. Elsisi, K. Mahmoud, M. Lehtonen and M.M.F. Darwish, *An Improved Neural Network Algorithm to Efficiently Track Various Trajectories of Robot Manipulator Arms*, *IEEE Access* **9** (2021) 11911.
- [147] R.A. Osornio-Ríos, *Identification of Positioning System for Industrial Applications using Neural Network*, *Journal of Scientific & Industrial Research* **76** (2017) 144.
- [148] M.W. Aslam, A.A. Zafar, M.N. Aslam, A.A. Bhatti, T. Hussain, M. Iqbal et al., *Particle swarm optimization based analysis to unlocking the neutrino mass puzzle using $SU(2)_L \times U(1)_Y \times A_4 \times S_2 \times Z_{10} \times Z_3$ flavor symmetry*, *Sci. Rep.* **15** (2025) 5129 [[2404.14917](#)].

- [149] M.W. Aslam and A.A. Zafar, *Optimizing Neutrino Mass Predictions with Neural Network Algorithm and $SU(2)_L \times U(1)_Y \times T_7 \times Z_{10}$ Symmetry*, *Int. J. Theor. Phys.* **64** (2025) 124.
- [150] M.W. Aslam, A.A. Zafar, M.N. Aslam and S. Saleem, *Optimizing neutrino mass predictions with competitive chaotic learning neural network algorithm and $SU(2)_L \times A_4 \times Z_3 \times Z_2$ symmetry*, *Modern Physics Letters A* **0** (0) 2550106.
- [151] M.K. Behera, S. Mishra, S. Singirala and R. Mohanta, *Implications of A_4 modular symmetry on neutrino mass, mixing and leptogenesis with linear seesaw*, *Phys. Dark Univ.* **36** (2022) 101027 [[2007.00545](#)].
- [152] M. Mirrashid and H. Naderpour, *Incomprehensible but intelligible-in-time logics: Theory and optimization algorithm*, *Knowledge-Based Systems* **264** (2023) 110305.
- [153] S. Antusch and V. Maurer, *Running quark and lepton parameters at various scales*, *JHEP* **11** (2013) 115 [[1306.6879](#)].
- [154] H. Okada and M. Tanimoto, *Towards unification of quark and lepton flavors in A_4 modular invariance*, *Eur. Phys. J. C* **81** (2021) 52 [[1905.13421](#)].
- [155] F. Björkeroth, F.J. de Anda, I. de Medeiros Varzielas and S.F. King, *Towards a complete $A_4 \times SU(5)$ SUSY GUT*, *JHEP* **06** (2015) 141 [[1503.03306](#)].
- [156] P. Mishra, M.K. Behera, P. Panda and R. Mohanta, *Type III seesaw under A_4 modular symmetry with leptogenesis*, *Eur. Phys. J. C* **82** (2022) 1115 [[2204.08338](#)].
- [157] S. Dawson, *Electroweak Symmetry Breaking and Effective Field Theory*, in *Theoretical Advanced Study Institute in Elementary Particle Physics: Anticipating the Next Discoveries in Particle Physics*, pp. 1–63, 12, 2017, DOI [[1712.07232](#)].
- [158] R.L. Workman, V.D. Burkert, V. Crede, E. Klempert, U. Thoma, L. Tiator et al., *Review of Particle Physics*, *Prog. Theor. Exp. Phys.* **2022** (2022) 083C01.
- [159] W. Rodejohann, *Neutrino-Less Double Beta Decay and Particle Physics*, *International Journal of Modern Physics E* **20** (2011) 1833 [[1106.1334](#)].
- [160] M. Mitra, G. Senjanović and F. Vissani, *Neutrinoless double beta decay and heavy sterile neutrinos*, *Nuclear Physics B* **856** (2012) 26 [[1108.0004](#)].
- [161] S.M. Bilenky and C. Giunti, *Neutrinoless Double-Beta Decay:.. a Brief Review*, *Modern Physics Letters A* **27** (2012) 1230015 [[1203.5250](#)].
- [162] W. Rodejohann, *Neutrinoless double-beta decay and neutrino physics*, *Journal of Physics G Nuclear Physics* **39** (2012) 124008 [[1206.2560](#)].
- [163] J.D. Vergados, H. Ejiri and F. Šimkovic, *Theory of neutrinoless double-beta decay*, *Reports on Progress in Physics* **75** (2012) 106301 [[1205.0649](#)].